Acta Pharmaceutica Sinica B 2026;16(1):322−336

Chinese Pharmaceutical Association
Institute of Materia Medica, Chinese Academy of Medical Sciences

Acta Pharmaceutica Sinica B

www.elsevier.com/locate/apsb
www.sciencedirect.com

ORIGINAL ARTICLE

USP10-mediated deubiquitination and activation of *KRAS* mutants promotes colorectal cancer *via* a novel USP10/KRAS positive feedback circuit

Tao Yuan[a,b,†], Weihua Wang[a,†], Ruilin Wu[a], Yue Liu[a], Junwei Fu[a], Jiamin Du[a], Meijia Qian[a], Jia'er Wang[a], Yubo Zhang[a], Wencheng Kong[c], Ronggui Hu[d], Tianhua Zhou[e], Qiaojun He[a,f], Bo Yang[a,g,*], Hong Zhu[a,d,*]

[a]*Institute of Pharmacology & Toxicology, Zhejiang Province Key Laboratory of Anti-Cancer Drug Research, College of Pharmaceutical Sciences, Zhejiang University, Hangzhou 310058, China*
[b]*Innovation Institute for Artificial Intelligence in Medicine, Zhejiang University, Hangzhou 310018, China*
[c]*Department of Gastroenterological Surgery, Hangzhou First People's Hospital, Hangzhou 310006, China*
[d]*Second Affiliated Hospital, Zhejiang University School of Medicine, Hangzhou 310009, China*
[e]*Department of Cell Biology, Zhejiang University School of Medicine, Hangzhou 310058, China*
[f]*Engineering Research Center of Innovative Anticancer Drugs, Ministry of Education, Hangzhou 310005, China*
[g]*School of Medicine, Hangzhou City University, Hangzhou 310015, China*

Received 22 February 2025; received in revised form 20 June 2025; accepted 15 July 2025

KEY WORDS

Deubiquitinase;
USP10;
KRAS;
Ubiquitination;
Phosphorylation;
Colorectal cancer;
Positive feedback circuit;
Therapeutic target

Abstract Kirsten rat sarcoma viral oncogene homolog (KRAS) mutation is associated with the poor prognosis of colorectal cancer (CRC) patients, but the therapeutic strategies targeting KRAS are limited, and novel intervention strategies are urgently needed. The dysfunction of deubiquitinases (DUBs) is widely involved in the progression of malignancy, and DUBs are considered ideal anti-tumor targets due to their well-defined structures and catalytic sites. In our study, through DUB inhibitors screening and liquid chromatography-tandem mass spectrometry (LC−MS/MS) analysis, we identified that ubiquitin-specific protease 10 (USP10) functions as a potent DUB regulating *KRAS* mutants' activity. Mechanistically, USP10 directly binds to and promotes *KRAS* variants' activity across different mutants by removing the latter's non-proteolytic ubiquitination chains mainly containing K6, K11, K27 and K29-linkage; while the activated *KRAS* mutants reciprocally upregulate USP10 levels by phosphorylating the

*Corresponding authors.
E-mail addresses: hongzhu@zju.edu.cn (Hong Zhu), yang924@zju.edu.cn (Bo Yang).
[†]These authors made equal contributions to this work.
Peer review under the responsibility of Chinese Pharmaceutical Association and Institute of Materia Medica, Chinese Academy of Medical Sciences.

https://doi.org/10.1016/j.apsb.2025.11.015

latter at Thr42/Ser337, therefore forming a positive feedback circuit and synergistically promoting *KRAS*-mutant CRC growth. Moreover, we found that USP10 is elevated in *KRAS*-mutant CRC tissues and depletion of USP10 preferentially impeded *KRAS*-mutant CRC growth *in vitro*/*in vivo*. Our findings not only uncover the critical roles of the USP10/KRAS positive feedback circuit in promoting *KRAS*-mutant CRC growth, but also offer novel therapeutic strategies for CRC patients harboring KRAS variants across different mutants by targeting USP10.

1. Introduction

Colorectal cancer (CRC) is the third most common cancer and the second leading cause of cancer death worldwide[1,2]. Despite great progress in targeted therapies, effective therapeutic strategies targeting Kirsten rat sarcoma viral oncogene homolog (*KRAS*) mutant CRC remain challenging[3-5]. Approximately 50% of CRC patients harbor *KRAS* mutations, and these patients show poor response to current chemotherapy and molecular-targeted drugs, resulting in poor prognosis[6-9]. Therefore, it is urgent to explore and develop novel and potent therapeutic strategies for CRC patients harboring *KRAS*-mutants.

Despite the success of $KRAS^{G12C}$ covalent inhibitors, sotorasib and adagrasib, which benefit those patients harboring $KRAS^{G12C}$ mutations[8,10-12], the incidence of $KRAS^{G12C}$ only accounts for ∼3% in CRC patients. Moreover, ∼50% of $KRAS^{G12C}$ patients rapidly develop acquired resistance after treatment with sotorasib[13-15], indicating most of the CRC patients cannot benefit from $KRAS^{G12C}$ covalent inhibitors. Son of sevenless 1 (SOS1) functions as the key effector promoting KRAS activity by modulating guanosine diphosphate/guanosine triphosphate (GDP/GTP) exchange and is considered an ideal target for KRAS intervention. However, BI-1701963, a previously considered promising SOS1 inhibitor, was ultimately terminated in phase I due to restraining normal KRAS activity, suggesting the impairment of normal KRAS activity leads to severe toxicity. Therefore, the intervention strategies of drugging *KRAS* mutants but sparing wild-type *KRAS* are urgently needed.

Ubiquitination modifications are the key processes in regulating KRAS activation, influencing the carcinogenic activity of KRAS by regulating its abundance or binding affinity to downstream effectors[7,16,17]. Ubiquitination modifications are primarily controlled by E3 ubiquitin ligases and deubiquitinating enzymes (DUBs), which are considered ideal drug targets due to their well-defined structures and catalytic active sites[18,19]. To date, several E3 ligases that regulate KRAS have been identified, including leucine zipper-like transcriptional regulator 1 (LZTR1)[20], beta-transducing repeat-containing protein (β-TRCP)[21] and WD40-repeat protein 76 (WDR76)[22], but developing the activators of these E3 enzymes remain a huge challenge. To date, the DUBs that directly regulate *KRAS* mutants remains less understood. A previous study reported that OTU domain-containing ubiquitin aldehyde-binding protein 1 (OTUB1) is involved in regulating KRAS[23], but OTUB1 modulates the membrane localization and activation of wild-type *KRAS*, not *KRAS* mutants, by inhibiting the enzymatic activity of the E2 enzymes ubiquitin-conjugating enzyme 13 (UBC13) and ubiquitin-conjugating enzyme E2 D3 (UBE2D3). Recently, ubiquitin-specific proteases 7 (USP7) was reported to stabilize *KRAS* and promote non-small cell lung cancer cell proliferation[24], but wild-type *KRAS* is also regulated by USP7, suggesting the potential risks of targeting USP7. So far, the specific DUBs that directly regulate *KRAS* mutants but spare wild-type *KRAS* remain unclear. Therefore, exploring DUBs that directly regulate *KRAS* mutants' activity while sparing wild-type *KRAS* is expected to provide potential therapeutic targets for *KRAS*-mutant CRC.

Ubiquitin-specific proteases 10 (USP10) belong to the USP family, the largest subfamily of DUBs. In recent years, the roles of USP10 in various malignant tumors have been gradually reported, revealing its dual functions. USP10 acts as a tumor suppressor by regulating Krüppel-like factor 4 (KLF4) stability and suppressing lung tumorigenesis[25]. In addition, USP10 antagonizes the transcriptional activity of c-Myc by preventing sirtuin 6 (SIRT6) ubiquitination and subsequent proteasomal degradation[26]. Conversely, USP10 also functions as an oncogenic factor. Weisberg et al.[27] found that USP10 promoted acute myeloid leukemia progression by deubiquitinating and stabilizing oncogenic FMS-like tyrosine kinase-3 (FLT3); inhibition of USP10 significantly induced the FLT3 ubiquitination and degradation. Consistent with these findings, our previous study also revealed that USP10 promotes hepatocellular carcinoma proliferation by preventing the ubiquitination and degradation of Yes-associated protein (YAP) and its paralog transcriptional coactivator with PDZ-binding motif (TAZ)[28]. Yuan et al.[29] found that USP10 is a critical DUB regulating Tumor protein 53 (TP53) stability by counteracting MDM2-mediated TP53 nuclear export and degradation. They demonstrated that USP10 suppresses cell proliferation in tumors with wild-type *TP53*, but promotes tumor growth in *TP53*-mutant tumor. These studies collectively indicate that the tumor-promoting or suppressing effect of USP10 is largely attributed to its substrates and the genetic context of the specific tumor. However, the roles of USP10 in *KRAS*-mutant CRC remain poorly understood.

In the current study, through a comprehensive screening of DUB inhibitors and liquid chromatography-tandem mass spectrometry (LC−MS/MS) analysis, we identified USP10 as a key promoter of *KRAS*-mutant CRC growth. Mechanistically, USP10 directly interacts with *KRAS* mutants and removes their non-proteolytic ubiquitination chains, predominantly containing Ub-K6, K11, K27, and K29 linkages. This deubiquitination enhances the activity of *KRAS* mutants. Conversely, activated *KRAS* mutants modulate USP10 protein levels and stability by promoting its phosphorylation at Tyr42 and Ser337, establishing a positive feedback circuit and synergistically driving *KRAS*-mutant CRC progression. Moreover, USP10 inhibition by RNA interference preferentially impedes the proliferation of *KRAS*-mutant CRC cells. Collectively, our findings identify USP10 as a novel regulator of oncogenic *KRAS* mutants and provide a potential therapeutic target for *KRAS*-mutant CRC.

2. Materials and methods

2.1. Cell culture

HEK-293T (RRID: CVCL_UE07), HCT-116 (RRID: CVCL_0291), HT-29 (RRID: CVCL_0320), SW480 (RRID: CVCL_0546), GP2d (RRID: CVCL_2450), SW837 (RRID: CVCL_1729), and SW620 (RRID: CVCL_0547) cells were originally obtained from the Cell Bank of Shanghai Institutes for Biological Sciences, Chinese Academy of Sciences (Shanghai, China). HEK-293T and SW480 cells were cultured in DMEM medium, while HT-29 and SW620 cells were maintained in RPMI-1640 medium and HCT-116 cells were maintained in McCoy's 5A medium. All cells were supplemented with 10% (*v*/*v*) FBS at 37 °C, in a humidified 5% CO_2 incubator, and routinely monitored negative for mycoplasma contamination. Authentication of the cell lines was confirmed by short tandem repeating profiling every year according to the standard of the international Cell Line Authentication Committee.

2.2. Antibodies and reagents

The antibodies against USP10 (#8501, RRID: AB_10949976), MEK (#4694, RRID: AB_10695868), p-MEK (#9154, RRID: AB_2138017), ERK (#4695, RRID: AB_390779), p-ERK (#4370, RRID: AB_2315112), and p-S/T (#9631, RRID: AB_330308) were purchased from Cell Signaling Technology (Danvers, MA, USA). Antibodies against HA (#db2603, RRID: AB_3451976) and GAPDH (#db106, RRID: AB_3271576) were purchased from Diagbio Biosciences (Hangzhou, China). Antibodies against KRAS (#sc-30, RRID: AB_627865), ubiquitin (Ub) (#sc-8017, RRID: AB_628423), and RAF1 (#sc-7267, RRID: AB_628196) were obtained from Santa Cruz Biotechnology (Dallas, TX, USA). Antibodies against MYC (#A00704, RRID: AB_914461) and FLAG (#A00187, RRID: AB_1720813) were obtained from GenScript (Nanjing, China). Antibodies against KRAS (#a12704, RRID: AB_2861676) were purchased from Abclonal (Wuhan, China). Protein synthesis inhibitor cycloheximide (#SBR00013) and puromycin(#P8833) were obtained from Sigma−Aldrich (St. Louis, MO, USA). Proteasome inhibitor MG132 (#S2619) and MAPK inhibitors PD98059 (#S1177) and SB203580 (#S1076) were obtained from Selleck (Houston, TX, USA). USP10 inhibitor Spautin-1 (#HY-12990) and other DUB inhibitors were purchased from MedChemExpress (NJ, USA). RAF1 RBD agarose beads (#ab211176) were purchased from Abcam (Cambridge, UK).

2.3. Gene transfection and lentivirus infection

JET-PRIME (Polyplus, Strasbourg, France, #114-01) was utilized to transfect indicated plasmids according to the manufacturer's instructions. The gene-specific shRNA sequences used in this study were as follows:

sh*USP10 #1*: GCCTCTCTTTAGTGGCTCTTT,
sh*USP10 #2*: GCTGTGGATAAACTACCTGAT.

2.4. Liquid chromatography-tandem-mass spectrometry (LC−MS/MS) analysis

To identify the potential proteins that interacted with KRAS, $KRAS^{G12V}$-Flag and vector were transfected into HEK-293T cells for 24 h. Then cells were lysed with RIPA lysis buffer (50 mmol/L Tris-Base, 150 mmol/L NaCl, 5 mmol/L EDTA, 1% NP40, 0.1% SDS, pH 7.4) and incubated with anti-Flag agarose beads to purify KRAS protein. The immunoprecipitated complexes were subjected to trypsin digestion for LC−MS/MS analysis. To identify the potential ubiquitin sites of $KRAS^{G12V}$, $KRAS^{G12V}$-Flag and HA-ub were transfected into HEK-293T cells for 24 h. Then cells were lysed with 4% SDS and incubated with anti-Flag agarose beads to purify ubiquitinated-KRAS protein. The immunoprecipitated complexes were subjected to trypsin digestion for LC−MS/MS analysis. LC−MS/MS analysis was performed by Jingjie PTM BioLab (Hangzhou, China). The operation protocol information, as well as procedures, was carried out according to the instructions provided by the company.

2.5. Immunoprecipitation and immunoblotting analysis

The immunoprecipitation (IP) assay and immunoblotting (IB) analysis were performed as previously described[28]. For endogenous immunoprecipitation, cell lysates were extracted, and the concentration of protein was measured by the BCA Protein Quantification Kit (YEASEN, 20201ES86). An equal amount of cell lysate was incubated with the agarose beads coupling anti-KRAS antibodies at 4 °C for overnight. The immunocomplexes were washed 8 times with RIPA lysis buffer (50 mmol/L tris-base, 150 mmol/L NaCl, 5 mmol/L EDTA, 1% NP40, 0.1% SDS, pH 7.4) followed by immunoblotting analysis.

2.6. Immunohistochemistry

The immunohistochemistry analysis was performed as described previously[30]. In brief, tissue slides were first de-paraffinized and immersed in PBS. The slides were heated in a microwave oven for 15 min in Citrate Antigen Retrieval buffer. After cooling to room temperature, the slides were incubated with 3% H_2O_2 to block endogenous peroxidase activity, and then incubated with 10% goat serum to block non-specific staining for 30 min, respectively. Subsequently, the slides were incubated with primary antibodies at 4 °C overnight and indicated secondary antibodies at room temperature for 1 h. After washing with PBS for 15 min, the slides were then exposed for 2−3 min to 3,3'-diaminobenzidine tetrahydrochloride (DAB) and rinsed off in deionized water to terminate the DAB reaction. The evaluation of the IHC staining was performed by a pathologist who was blind from the gene information of these patients.

2.7. Cell proliferation and colony formation assays

CRC cells infected with the indicated lentivirus were seeded at 1000 cells/well in 96-well plates, and the optical density value was measured every day. The cell proliferation was assessed by sulforhodamine B (SRB) assay, in brief, the cell plates were fixed with 100 μL 10% trichloroacetic acid solution (pre-cooled at 4 °C) each well for 1 h at 4 °C, then the supernatant was discarded, and the cells were washed three times with double-distilled water and then dried. Subsequently, 100 μL 1% SRB staining solution was added to each well, and the plates were left at room temperature for 20 min. After that, the wells were washed clean with 1% glacial acetic acid and dried. Finally, 100 μL of tris-base solution was added to each well to dissolve the SRB staining solution bound to the cells. The cell plates were then placed on a room temperature shaker for 20 min, and the absorbance was measured at a wavelength of 515 nm. For colony formation assay, CRC cells infected with indicated shRNA were plated with 1000 cells/well in

6-well plates for 2 weeks, and were stained by SRB to count the number of colonies.

$$\text{Inhibition rate (IR, \%)} = (\text{Absorbance}_{\text{control}} - \text{Absorbance}_{\text{treatment}}) / \text{Absorbance}_{\text{control}} \times 100 \quad (1)$$

$$\Delta \text{ Inhibition rate } (\Delta\text{IR}) = \text{IR}_{\text{Mut}} - \text{IR}_{\text{WT}} \quad (2)$$

2.8. Real-time PCR

Total RNA was freshly extracted by TRIzol (Invitrogen, Carlsbad, CA, USA). Using TransScript One-Step gDNA Removal and cDNA Synthesis SuperMix Kit (Transgen) to carry out reverse transcription PCR and acquire cDNA. Subsequently, SYBR-Green was applied to real-time PCR analysis. The sequences of primers were used as follows:

USP10, forward primer: ATTGAGTTTGGTGTCGATGAA GT;

USP10, reverse primer: GGAGCCATAGCTTGCTTCTTTAG;

KRAS, forward primer: ACAGAGAGTGGAGGATGCTTT;

KRAS, reverse primer: TTTCACACAGCCAGGAGTCTT;

GAPDH, forward primer: GGAGCGAGATCCCTCCAAAAT;

GAPDH, reverse primer: GGCTGTTGTCATACTTCTCAT GG.

2.9. In vitro deubiquitination assay

Flag-tagged KRAS and HA-tagged ubiquitin were transfected into HEK-293T cells. After 24 h, cells were harvested and lysed with 4% SDS buffer, and the extracts were incubated with anti-flag beads at 4 °C for overnight. The poly-ubiquitinated KRAS protein was incubated with bacterial-expressed rhUSP10 for 2 h at 37 °C *in vitro*, followed by immunoblotting analysis.

2.10. Antitumor activity in vivo

BALB/c-Nude mice (RRID: IMSR_RJ: BALB-C-NUDE, 4−5 weeks) were purchased from GemPharmatech Co., Ltd. (Jiangsu, China) and maintained in a pathogen-free animal facility. All animal experiments were performed according to the regulations of the Institutional Animal Care and Use Committee (IACUC). The protocols for the animal study and field sample permit were approved by the Innovation Institute for Artificial Intelligence in Medicine of Zhejiang University (approval number: DW22071101, China). BALB/c-Nude mice were subcutaneously injected with 1×10^6 CRC cells in 200 μL medium. When tumor volume reached 50 mm^3, these mice were randomly divided into two groups and underwent intratumor injection of the scramble or shUSP10 lentivirus every two days. At the endpoint of the experiment, the mice were humanely euthanized *via* cervical dislocation. Tumor volume (V) was calculated as Eq. (3):

$$V = (\text{Length} \times \text{Width}^2)/2 \quad (3)$$

2.11. Patient-derived xenograft models

The patient-derived xenograft study had obtained informed consent from all participants and was approved by the Ethics Committee of the Hangzhou First People's Hospital (ethics approval license: KY-20220105-0011-01, China). The gender, age, and body weight of participants are not variables in our study. The tumor specimens from *KRAS*-mutant CRC patient were cut into pieces of 1 mm^3 under sterile conditions and subcutaneously transplanted into BALB/c-Nude mice. When tumor volume reached around 50 mm^3, these mice were randomly divided into two groups and underwent intratumor injection of the scramble or shUSP10 lentivirus every two days. At the endpoint of the experiment, the mice were humanely euthanized *via* cervical dislocation. Tumor volume was calculated as described previously.

2.12. In vitro ubiquitin 7-amido-4-methylcoumarin (Ub-AMC) assay

293T cells transfected with vector or USP10-WT/C424A-Flag were lysed in RIPA lysis buffer (50 mmol/L tris-base, 150 mmol/L NaCl, 5 mmol/L EDTA, 1% NP40, 0.1% SDS, pH 7.4), and protein quantification was measured by BCA Protein Quantification Kit (YEASEN, 20201ES86). An equal amount of cell lysate was incubated with anti-Flag sepharose for 2 h at 4 °C. The immunocomplexes were washed 6 times with RIPA lysis buffer and then subjected to an *in vitro* Ub-AMC assay. For the *in vitro* Ub-AMC assay, the equal immunocomplexes were incubated in reaction buffer (50 mmol/L tris-HCl, 5 mmol/L $MgCl_2$, 2 mmol/L DTT, 2 mmol/L ATP, pH 7.5) at 37 °C for 1 h. Reactions were initiated by adding 2 μmol/L Ub-AMC (Boston Biochem, #U-550). Fluorescence levels were measured continuously at 25 °C using a Tecan Spark Microplate Reader at an excitation wavelength of 345 nm and an emission wavelength of 445 nm.

2.13. Statistical analysis

Numbers of biological replicates in different experiments are included in each figure legend and supplementary figure legend. No statistical methods were used to predetermine sample sizes, but our sample sizes are similar to those generally employed in this field. No codes have been used in our study. All experiments were randomized and blinded where possible, and no data were excluded. All experiments were repeated at least three times in our study, and the independent experiment results are presented as the mean ± standard deviation (SD) or mean ± standard error of mean (SEM). Two-tailed unpaired Student's *t*-test was used for calculating statistical significance of two groups, while one-way ANOVA was used when multiple groups were compared. All statistical results were conducted using GraphPad Prism (RRID: SCR_002798). Differences in means were considered significant when $P < 0.05$ ($^*P < 0.05$, $^{**}P < 0.01$, and $^{***}P < 0.001$).

3. Results

3.1. Identification of USP10 as an essential regulator of KRAS mutants

Given *KRAS* mutation contributing to its robust tumor-promoting activities, we conducted paired HT-29 cell lines harboring $KRAS^{WT/G12C/G12D/G12V}$ ($KRAS^{WT/Mut}$) and performed a whole-cell phenotypic screen to identify the underlying DUBs that are essential for *KRAS* mutant but not available to *KRAS* wild-type CRC (Fig. 1A and Supporting Information Fig. S1A). We evaluated DUB inhibitors for their selective activity in inhibiting the

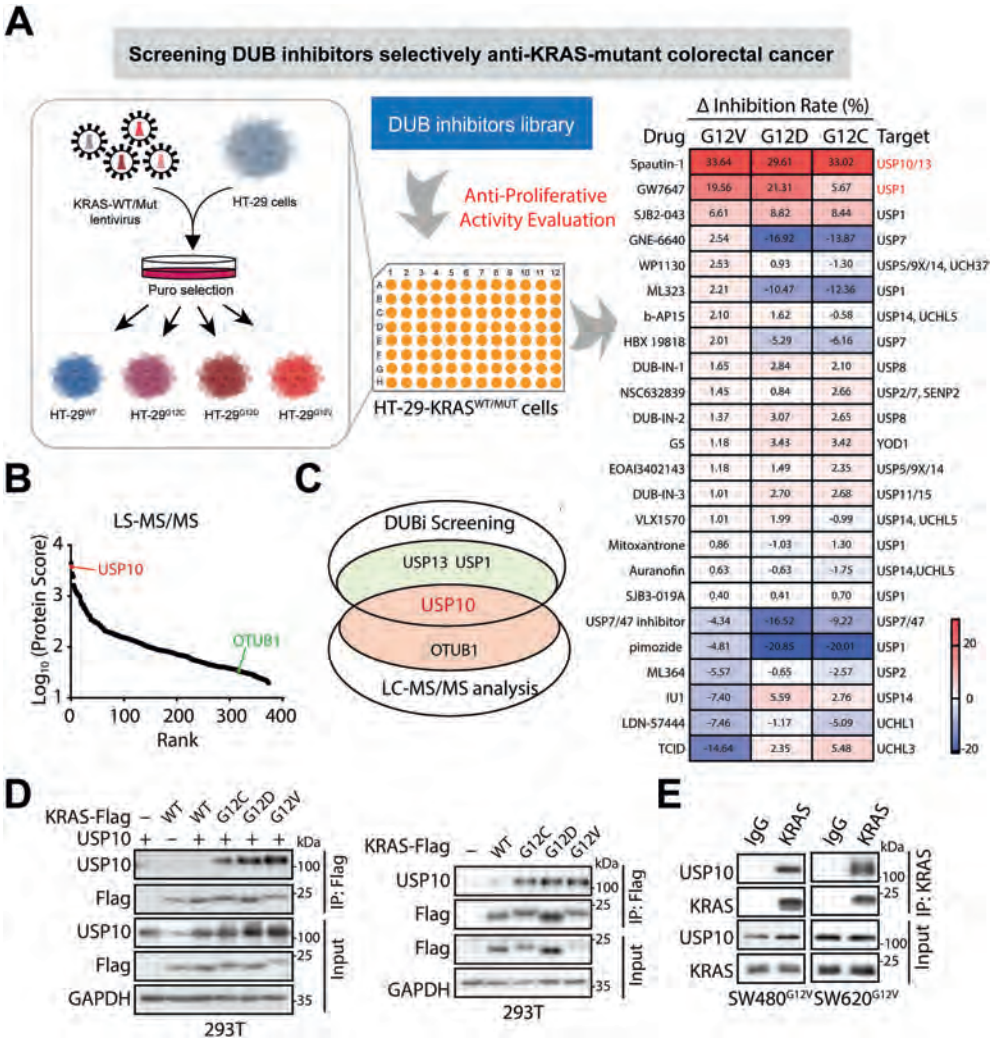

Figure 1 Identification of USP10 as an essential regulator of *KRAS* mutants. (A) The schematic diagram of DUB inhibitors (DUBi) library screening and identification Spautin-1 selectively inhibiting *KRAS*-mutant CRC cell growth. HT-29 cells were infected with the lentivirus that stably over-expressed *HT-29-KRAS*$^{WT/G12C/G12D/G12V}$ (*HT-29-KRAS*$^{WT/Mut}$) and screened by using puromycin, then these cells were seeded with 1000 cells/well in 96-well plates, and then were treated with 10 μmol/L DUB inhibitor for 72 h, followed by SRB assays. (B) The underlying proteins interacting with oncogenic KRAS were identified by LC−MS/MS. HEK-293T cells were transfected with KRAS^{G12V}-Flag and vector for 24 h, then cells were lysed with RIPA lysis buffer and incubated with anti-Flag agarose beads. The immunoprecipitated KRAS-Flag was captured using SDS-PAGE and the gel was subjected to trypsin digestion for LC−MS/MS analysis. (C) The Venn diagram illustrate the potential targets that are involved in oncogenic KRAS-induced cell proliferation and interact with *KRAS* mutants. (D) USP10 predominantly interacts with mutant *KRAS in vivo.* HEK-293T cells were co-transfected with indicated expression plasmids and the cell lysates were subjected to IP assays. (E) USP10 interacts with *KRAS* mutants at endogenous levels. Cell lysates of SW480 and SW620 were incubated with the affinity gel conjugated with KRAS antibody. Proteins retained on the affinity gel were subjected to IB analysis.

proliferation of *HT-29-KRAS*^{Mut} cells by screening DUB inhibitors library. From this screen, Spautin-1, previously reported as a USP10/USP13 inhibitor, emerged as a distinct hit, selectively impeding the proliferation of *HT-29-KRAS*^{Mut} cells (Fig. 1A). Additionally, LC−MS/MS analysis identified more than 300 proteins interacting with *KRAS* mutants, including OTUB1, a DUB reported to modulate the membrane localization of *KRAS* wild-type but not that of *KRAS* mutants by inhibiting E2 enzymes UBC13 and UBE2D3 activity, indicating the reliability of LC−MS/MS results (Supporting Information Table S1). Among these identified proteins, the protein score of USP10 ranks second only to that of KRAS (Fig. 1B). Together, the results of the DUB inhibitors screening and LC−MS/MS analysis suggest that USP10 functions as a potential DUB regulating *KRAS* mutants (Fig. 1C).

To clarify whether USP10 functions as a DUB directly regulating *KRAS* mutants, we first examined the interaction between *USP10* and *KRAS* mutants/wild-type. As shown in Fig. 1D, the substantial interaction between *USP10* and *KRAS* mutants has been observed while there is a very weak binding between *USP10* and *KRAS* wild-type; moreover, the interaction between USP10 and KRAS was independent of USP10's enzymatic activity (Fig. S1B), Meanwhile, the endogenous interaction between USP10 and *KRAS* mutants in *KRAS*-mutant CRC cells has also been confirmed by co-immunoprecipitation assays (Fig. 1E and Fig. S1C). Collectively, these data

demonstrated that USP10 is a *bona fide* binding protein of KRAS.

3.2. *USP10 positively regulates KRAS mutants' activity*

Given that USP10 interacts with *KRAS* mutants, we sought to determine whether USP10 regulates the turnover of *KRAS* mutants. Initially, we investigated the effect of USP10 on *KRAS* mutants' levels and found that *USP10* knockdown did not affect KRAS protein levels (Fig. 2A). Subsequently, we introduced wild-type *USP10* and its enzymatic mutant USP10-CA and found that USP10-CA almost lost whole enzymatic activity, which are consistent with the observations in other studies (Supporting Information Fig. S2A)[28,31,32]. More importantly, Overexpression of USP10 and USP10-CA failed to pose any effect on KRAS protein levels (Fig. 2B). Meanwhile, we also examined the effect of USP10 and its inhibitor Spautin-1 on *KRAS* mRNA levels. As shown in Fig. 2C and Fig. S2B and S2C, neither depletion of USP10 nor overexpression of USP10-WT/CA or its inhibitor affects *KRAS* mRNA levels. These results indicate that USP10 does not regulate the transcriptional levels and turnover of *KRAS* mutants.

Subsequently, we further examined the effect of USP10 on KRAS activity by measuring its classical downstream MAPK pathway. As shown in Fig. 2D and Fig. S2D, depletion of USP10 remarkably decreased the phosphorylation of MAPK kinase (MEK) and extracellular signal-regulated kinase (ERK), suggesting the inhibition of the MAPK pathway. Additionally, we also introduced USP10 inhibitor Spautin-1 and found Spautin-1 also significantly suppressed the MAPK pathway (Fig. 2E). Correspondingly, overexpression of USP10 promoted MAPK pathway activation, whereas its enzymatic mutant USP10-CA did not have similar effect (Fig. 2F). Meanwhile, we further investigated the effect of USP10 knockdown on PI3K−AKT signaling, another classical downstream pathway of KRAS. As shown in Fig. S2E, depletion of USP10 remarkably downregulated p-AKT levels, indicating the significant inhibition of *USP10* knockdown on PI3K−Akt signaling.

Taken together, these results suggest that USP10 positively regulated the activity of *KRAS* mutants, but imposed minimal effect on their protein levels.

3.3. *USP10 directly deubiquitinates KRAS mutants in an enzymatic activity-dependent manner*

The aforementioned data demonstrated that USP10 interacts with *KRAS* mutants and positively regulates their activity. Considering USP10 functions as a DUB, we hypothesized that USP10 might promote MAPK activation by deubiquitinating *KRAS* mutants; therefore, we examined the effect of *USP10* on *KRAS* mutants' ubiquitination levels. As shown in Fig. 3A and B and Fig. S2F, overexpression of wild-type *USP10*, but not its enzymatic mutant

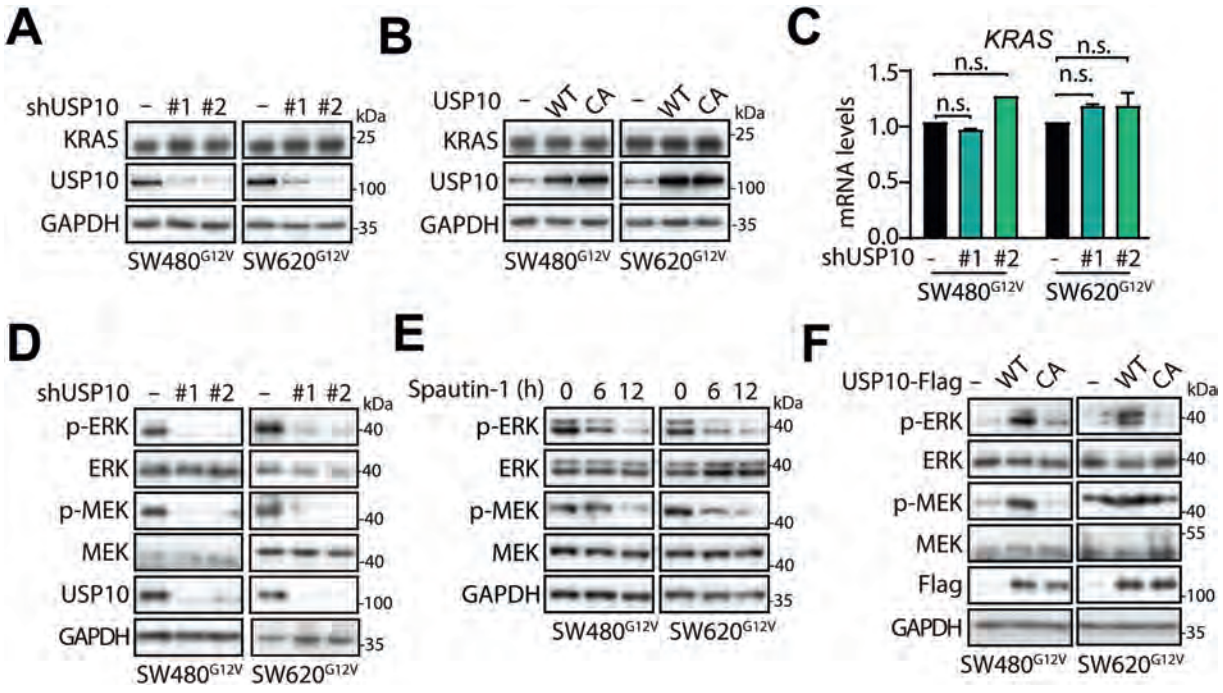

Figure 2 USP10 positively regulates *KRAS* mutants' activity. (A) Depletion of USP10 posed little effect on KRAS protein levels. SW480 and SW620 cells were infected with the lentivirus encoding the indicated shRNA, and the cell lysates were subjected to IB analysis. (B) Overexpression of USP10 posed little effect on KRAS protein levels. SW480 and SW620 cells were transfected with USP10-WT or USP10-CA, and the cell lysates were subjected to IB analysis. (C) Depletion of USP10 posed little effect on *KRAS* mRNA levels. SW480 and SW620 cells were infected with the lentivirus encoding the indicated shRNA, and cell lysates were subjected to real-time PCR assays (Mean ± SD, $n = 3$). (D) Depletion of USP10 remarkably sustained MAPK signaling. SW480 and SW620 cells were infected with indicated sh*RNA*s, and the cell lysates were subjected to IB analysis. (E) USP10 inhibitor Spautin-1 significantly suppressed MAPK signaling. SW480 and SW620 cells were treated with 25 μmol/L Spautin-1 for the indicated time, and the cell lysates were subjected to IB analysis. (F) Overexpression of USP10 significantly promoted MAPK signaling in an enzymatic activity-dependent manner. SW480 and SW620 cells were transfected with the indicated plasmid, and the cell lysates were subjected to IB analysis. n.s., $P > 0.05$.

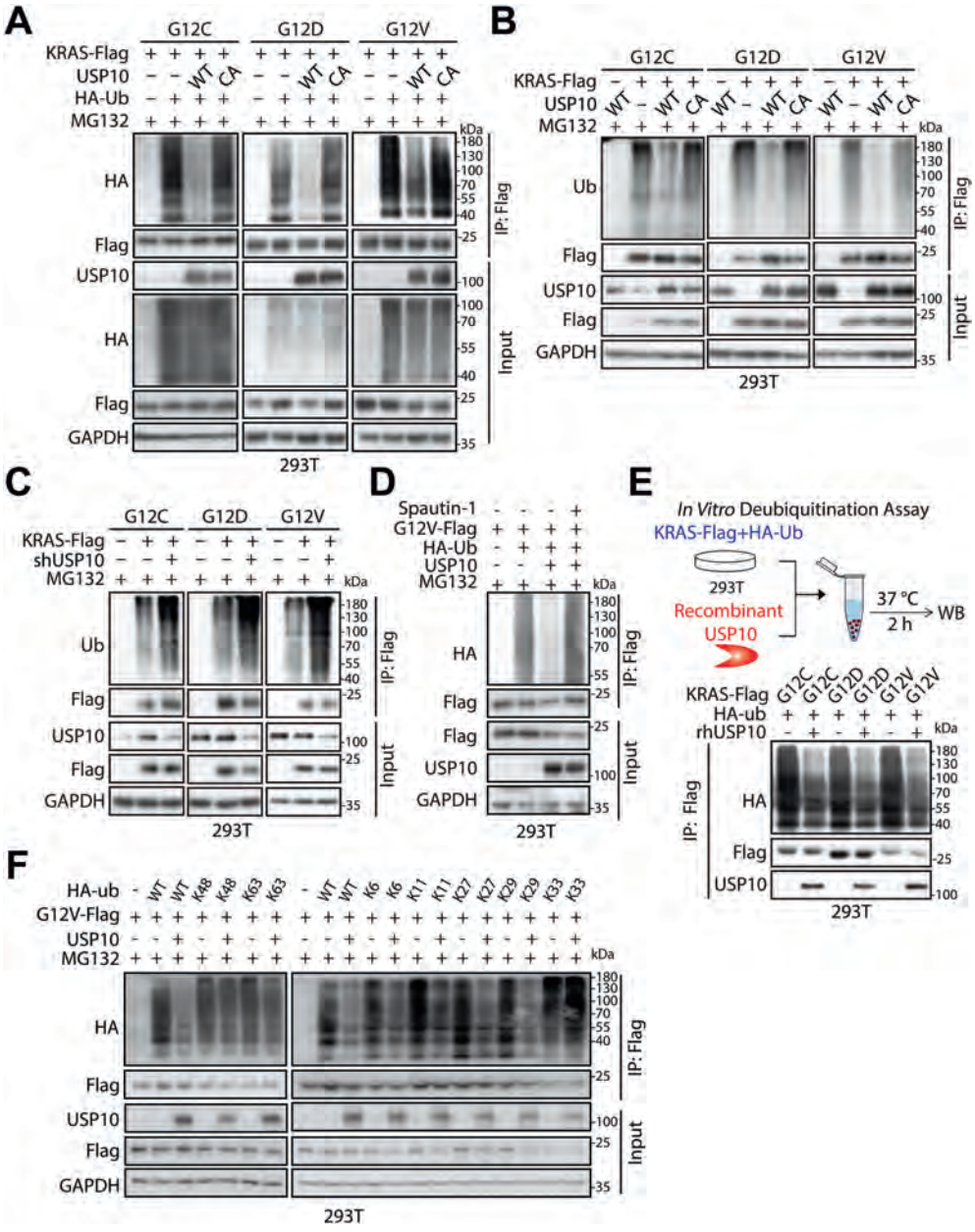

Figure 3 USP10 directly deubiquitinates KRAS in an enzymatic activity-dependent manner. (A, B) Overexpression of USP10-WT, but not USP10-CA, significantly decreases *KRAS* mutants' ubiquitination levels. Cells transfected with the indicated plasmids were treated with MG132 (10 μmol/L, 8 h) before harvested. Total cell lysates were immunoprecipitated with anti-Flag affinity gels, then the proteins remaining on gels were subjected to IB analysis. (C) Depletion of USP10 dramatically increased *KRAS* mutants' ubiquitination. HEK-293T cells infected with control/USP10 shRNA were transfected with the indicated plasmids and treated with MG132 (10 μmol/L, 8 h) before harvested. Cell lysates were immunoprecipitated with anti-Flag affinity gels, and the proteins remaining on gels were subjected to IB analysis. (D) USP10 inhibitor Spautin-1 significantly increased *KRAS* mutants' ubiquitination. HEK-293T cells transfected with the indicated plasmids were treated with MG132 (10 μmol/L, 8 h) and Spautin-1 (50 μmol/L, 10 h) before harvested. Cell lysates were immunoprecipitated with anti-Flag affinity gels, then the protein remaining on gels were immunoblotted with the indicated antibodies. (E) Bacterial-expressed recombinant human USP10 (rhUSP10) effectively removed the polyubiquitination of *KRAS* mutants *in vitro*. HEK-293T cells were transfected with indicated expression plasmids and cell lysates were incubated with anti-Flag affinity gel for overnight. Then, proteins retained on anti-Flag affinity gel were incubated with rhUSP10 in 37 °C for 2 h, followed by IB assays. (F) Overexpression of USP10 efficiently removes the K6-, K11-, K27- and K29-linked polyubiquitin chains of *KRAS* mutants. Cells transfected with the indicated plasmids were treated with MG132 (10 μmol/L, 8 h) before harvested. Total cell lysates were immunoprecipitated with anti-Flag affinity gels, then the proteins remaining on gels were immunoblotted with the indicated antibodies.

CA, significantly decreased *KRAS* mutants' ubiquitination levels, indicating USP10 regulated KRAS ubiquitination levels in an enzymatic activity-dependent manner. Conversely, depletion of USP10 remarkably increased *KRAS* mutants' polyubiquitylation levels (Fig. 3C and Fig. S2G). Additionally, we tested the effect of Spautin-1 on KRAS ubiquitination levels. As shown in Fig. 3D, Spautin-1 reversed the decreased ubiquitination levels of *KRAS* mutants induced by USP10 overexpression. These results collectively suggest that USP10 negatively regulates *KRAS* mutants' ubiquitination levels.

To further demonstrate the deubiquitination activity of USP10 towards *KRAS* mutants, we performed *in vitro* deubiquitination assays using a cell-free system. We found that recombinant USP10 protein effectively removed the polyubiquitin chains from *KRAS* mutants *in vitro* (Fig. 3E). Subsequently, we investigated the types of ubiquitin chains that USP10 removes from *KRAS* mutants. As shown in Fig. 3F, USP10 primarily removed the non-proteolytic ubiquitination chains, including Ub-K6, K11, K27 and K29-linked chains. To further identify the ubiquitin sites of *KRAS* mutants, we performed LC−MS/MS analysis and found that K42, K128, K147 and K176 are the underlying ubiquitin sites of KRAS (Supporting Information Table S2). Subsequently, we constructed the ubiquitin site mutants of *KRAS* (*KRAS*-4KR/*KRAS-K42R*/*K128R*/*K147R*/*K176R*) and performed *in vivo* ubiquitination assays. As shown in Fig. S2H, USP10 overexpression significantly removed the polyubiquitination chains of KRAS, while posing minimal effect on *KRAS*-4KR, demonstrating *K42*, *K128*, *K147* and *K176* are the main ubiquitin sites of *KRAS* regulated by USP10.

These results demonstrated that USP10 deubiquitinates *KRAS* mutants by removing non-proteolytic ubiquitination chains, main including K6, K11, K27 and K29-linked ubiquitin in an enzymatic activity-dependent manner.

3.4. USP10 knockdown significantly suppresses KRAS-mutant CRC growth in vitro and in vivo

Given that USP10 positively regulates *KRAS* mutants' activity, we next investigated the roles of USP10 in *KRAS*-mutant CRC growth. As shown in Fig. 4A and B and Supporting Information Fig. S3A-S3D, depletion of USP10 remarkably inhibited the proliferation and colony formation of *KRAS* mutant CRC, indicating that *USP10* knockdown significantly suppresses *KRAS*-mutant CRC growth *in vitro*. Subsequently, we also performed an *in vivo* xenograft experiment to investigate the effect of USP10 on the growth of *KRAS*-mutant CRC xenografts. As shown in Fig. 4C−E and Supporting Information Table S3, depletion of USP10 significantly inhibited the tumor growth of SW480 and SW620 xenografts, as reflected by the decrease in relative tumor volume and tumor weight. Subsequently, we further analyzed the intratumor proteins and found that USP10 depletion significantly downregulated intratumor p-MEK and p-ERK levels (Fig. 4F).

To further investigate USP10's impact on *KRAS*-mutant CRC growth in a preclinical setting, we constructed a primary patient-derived xenograft (PDX) from a clinical *KRAS*-mutant colorectal cancer patient (Fig. 4G). As shown in Fig. 4H−J and Table S3, similar results were obtained, indicating that USP10 depletion inhibited *KRAS*-mutant CRC xenografts growth by restraining KRAS activity. Collectively, these results confirmed that USP10 plays a crucial role in promoting *KRAS* mutant CRC growth *in vitro* and *in vivo*.

To gain further insight into the relevance between USP10 and CRC pathogenesis, we analyzed USP10 levels in normal and tumor tissues of CRC patients by using the Cancer Genome Atlas Program (TCGA) database. As shown in Fig. 4K, CRC tumor tissues exhibited higher USP10 levels than normal tissues. Additionally, we collected clinical CRC patient samples and performed the IHC assays to comparatively investigate USP10 expression in tumor versus adjacent normal tissues. As shown in Fig. 4L, USP10 expression levels were significantly higher in tumor tissue compared to adjacent normal tissues, consistent with the results obtained from the TCGA database. Moreover, we found that high USP10 levels inversely correlated with the overall survival and relapse-free survival of CRC patients (Fig. 4M and Fig. S3E), highlighting that USP10 is involved in the malignant progression of CRC and is closely associated with the poor prognosis of CRC patients.

3.5. KRAS mutants upregulate USP10 levels and stability by promoting the phosphorylation of USP10 at Tyr42 and Ser337

The significant differences in binding amount between *USP10* and *KRAS* wild-type/mutant led us to hypothesize that USP10 plays distinct roles in *KRAS* wild-type and mutant CRC. To test this hypothesis, we collected the clinical samples of *KRAS* wild-type/mutant CRC patients and compared the expression levels of USP10 by performing immunohistochemistry (IHC) assays. As shown in Fig. 5A, *KRAS*-mutant CRC samples exhibited higher USP10 levels compared to *KRAS* wild-type samples, suggesting that *KRAS* mutants may function as a driver promoting USP10 overexpression in *KRAS*-mutant CRC.

To decipher the underlying molecular mechanism of USP10 overexpression in *KRAS*-mutant CRC, we examined the effect of *KRAS* wild-type/mutant on USP10 levels. As shown in Fig. 5B, overexpression of *KRAS* mutants, but not wild-type *KRAS*, remarkably upregulated USP10 protein levels, indicating that *KRAS* mutants specifically enhance USP10 protein levels. To further investigate whether *KRAS* mutants mediated USP10 upregulation at the posttranslational levels or transcriptional levels, we next examined the effect of *KRAS* mutants/wild-type on *USP10* mRNA levels. As shown in Supporting Information Fig. S4A, neither *KRAS* mutants nor *KRAS* wild-type influenced *USP10* mRNA levels, implying that *KRAS* mutants upregulated USP10 levels at the posttranslational levels rather than the transcriptional levels.

Phosphorylation cascade signaling is the key process by which *KRAS* mutants regulate downstream proteins; we therefore examined the effect of *KRAS* mutants on USP10 phosphorylation levels. As shown in Fig. 5C, overexpression of *KRAS* mutants, but not *KRAS* wild-type, significantly increased the phosphorylation levels of USP10; moreover, this effect could be weakened by MEK inhibitor PD98059 (Fig. 5D), indicating that the upregulation of USP10 phosphorylation levels is mediated by the MAPK signaling pathway. Subsequently, we attempted to identify the underlying kinase-mediated KRAS upregulating USP10 phosphorylation. Given the MEK inhibitor can weaken the effect of *KRAS* mutants-induced USP10 phosphorylation upregulation, we focused on the kinases associated with the RAF−MEK−ERK pathway. We performed LC−MS/MS analysis and found Mitogen-activated protein kinase 1 (MAPK1/ERK2) interacts with USP10 (Supporting Information Table S4). Subsequent co-immunoprecipitation assay also demonstrated the interaction between USP10 and MAPK1 (Fig. S4B). More importantly, we

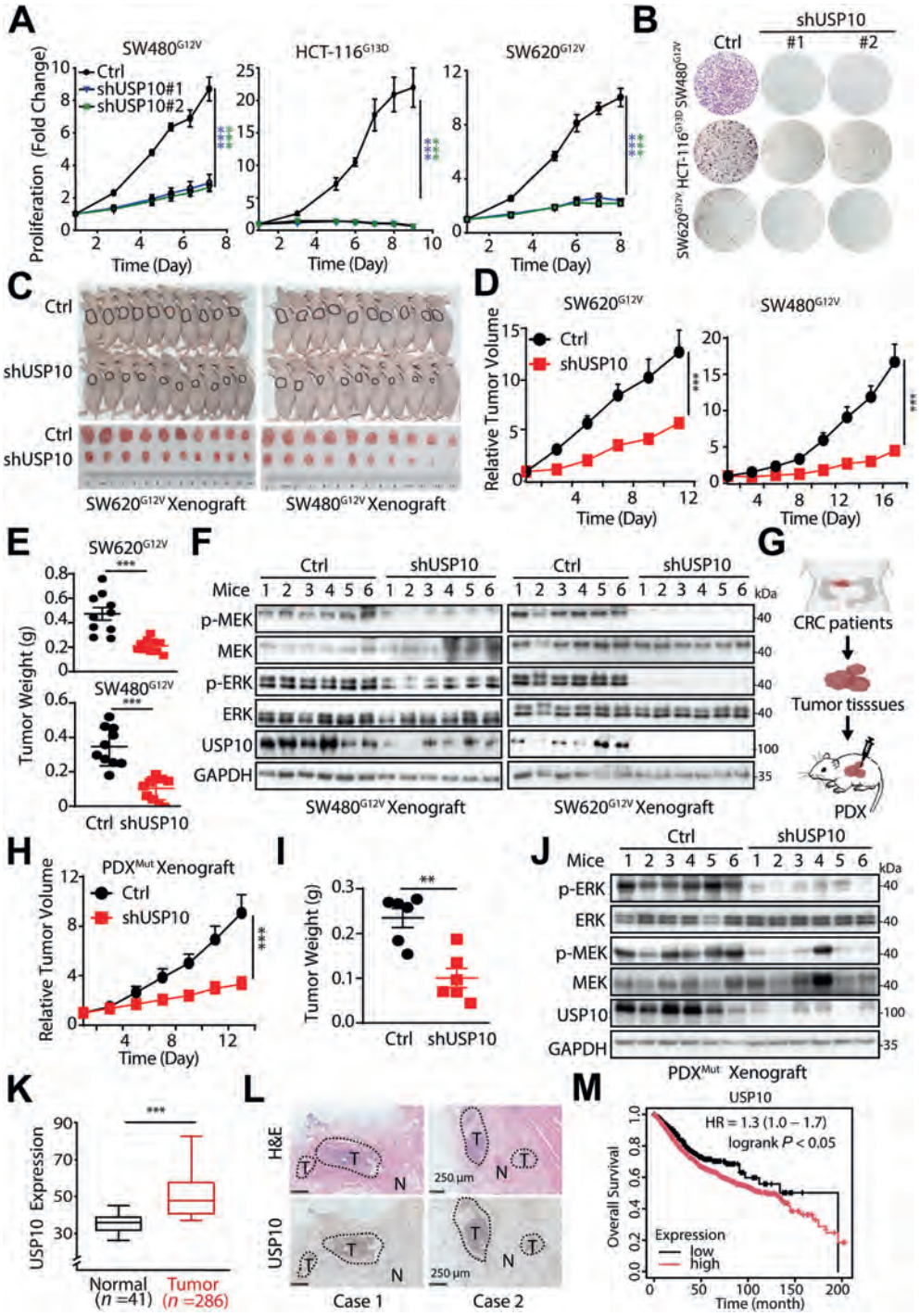

Figure 4 USP10 knockdown significantly suppresses *KRAS*-mutant CRC growth *in vitro* and *in vivo*. (A, B) Depletion of USP10 suppressed the proliferation of *KRAS*-mutant CRC cells *in vitro*. SW620, SW480 and HCT-116 cells were infected the lentivirus that encoding control/USP10 shRNA, followed by cell proliferation assays and colony formation assays (mean ± SD; $n = 3$). (C−E) Depletion of USP10 significantly arrested the growth of *KRAS*-mutant CRC xenografts *in vivo*. (C) The bearing-tumor mice and tumor images. (D) The relative tumor volume of the indicated groups. (E) The tumor weight of indicated groups (mean ± SEM; $n = 10$/group). (F) USP10 knockdown remarkably inhibited intratumor MAPK signaling. Immunoblot analysis of related protein levels in SW480 xenografts and SW620 xenografts. (G) The schematic diagram of PDX models. (H, I) Depletion of USP10 significantly inhibited the growth of *KRAS*-mutant CRC PDX *in vivo* (mean ± SEM; $n = 6$/group). (H) The relative tumor volume of indicated groups. (I) The tumor weight of indicated groups. (J) USP10 knockdown remarkably restrained intratumor MAPK signaling. Immunoblot analysis of related protein levels in PDXs. (K) USP10 levels in tumor tissues are significantly higher than those of in normal tissues in CRC patients. (L) USP10 is significantly overexpressed in tumor tissue compared to normal tissue in CRC patients. Representative section of H&E staining and USP10 staining in CRC patient tissues. T: tumor tissues; N: para-carcinoma tissues; scale bars: 250 μm. (M) USP10 level is inversely correlated with the overall survival of CRC patients. The correlation analysis between USP10 expression and overall survival of colorectal cancer patients in the Kaplan−Meier Plotter database (split by the best cutoff). $^{**}P < 0.01$; $^{***}P < 0.001$.

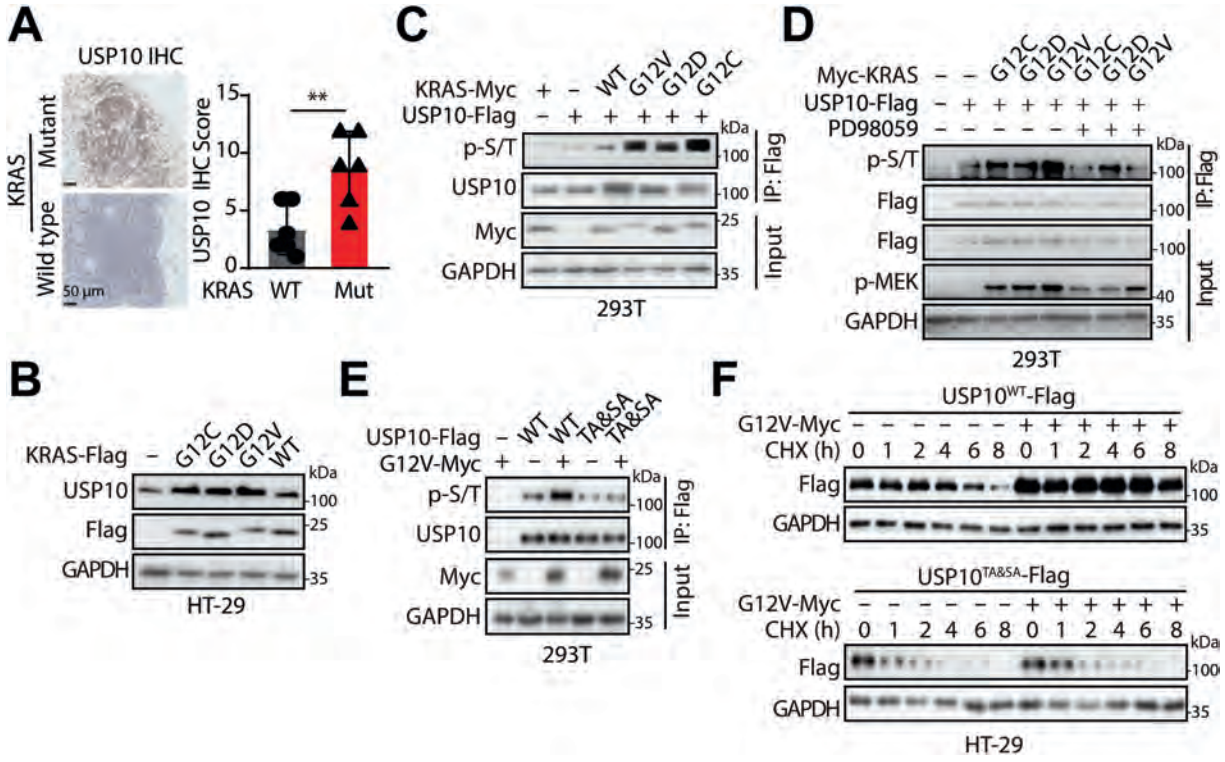

Figure 5 *KRAS* mutants upregulates USP10 levels and stability by promoting the phosphorylation of USP10 at Tyr42 and Ser337. (A) *KRAS*-mutant CRC patients displayed higher USP10 levels compared to *KRAS* wild-type patients. Immunohistochemistry (IHC) staining of intratumor USP10 in *KRAS* mutants/wild-type CRC patients (mean ± SD, $n = 6$). (B) Overexpression of *KRAS* mutants significantly upregulated USP10 protein levels. HT-29 cells were transfected with the indicated plasmids and cell lysates were subjected to IB assays. (C) Overexpression of *KRAS* mutants, not *KRAS* wild-type, significantly promoted USP10 phosphorylation. HEK-293T cells transfected with indicated plasmids were immunoprecipitated with anti-Flag agarose beads and the protein remaining on anti-Flag agarose beads were subjected to IB assays. (D) MAPK inhibitor PD98059 reversed the upregulation of USP10 phosphorylation induced by *KRAS* mutants. HEK-293T cells transfected with indicated plasmids were treated with DMSO, PD98059 (10 μmol/L) for 24 h before harvested, then cell lysates were immunoprecipitated with anti-Flag agarose beads and immunoblotted with the indicated antibody. (E) T42 and S337 are the main phosphorylation sites of USP10 regulated by *KRAS* mutants. HEK-293T cells transfected with indicated plasmids were immunoprecipitated with anti-Flag agarose beads and the protein remaining on anti-Flag agarose beads was subjected to IB assays. TA&SA: T42A&S337A. (F) *KRAS* mutants significantly increased the protein levels and stability of USP10-WT, but not USP10-T42A&S337A. HT-29 cells expressing USP10-WT/TA&SA were infected with lentivirus encoding Vector or $KRAS^{G12V}$-Myc and treated with 20 μg/mL CHX for indicated time and the cell lysates were immunoblotted with the indicated antibody. TA&SA: T42A&S337A. $^{**}P < 0.01$.

found MAPK1 overexpression promoted USP10 phosphorylation (Fig. S4B), and MAPK1 depletion attenuated the upregulation of USP10 phosphorylation induced by *KRAS* mutants to a certain extent (Fig. S4C). These data collectively demonstrated *KRAS* mutants upregulate USP10 relying on MAPK1 at least in part.

Next, we sought to identify the specific phosphorylation sites mediated *KRAS* mutants upregulating USP10. Previous studies have shown that USP10 is primarily phosphorylated at Thr42 (T42), Ser76 (S76) and Ser337 (S337) [29,33]. Among these phosphorylation sites, Thr42 and Ser337 are known to affect USP10 stability[29], while Ser 76 affects USP10's activity[33]. We mutated these three phosphorylation sites to Alanine (Ala), thereby abolishing their phosphorylation. Interestingly, co-mutation at T42 and S337 (TA&SA) abolished the *KRAS* mutants-induced upregulation of USP10 phosphorylation, while the Ser 76 mutation did not have a similar effect (Fig. 5E and Fig. S4D), indicating Thr42 and Ser337 are the primary phosphorylation sites through which *KRAS* mutants upregulate USP10. We also investigated whether the phosphorylation at these sites affects USP10's binding and deubiquitinating activity towards KRAS. As shown in Fig. S4E and S4F, the co-mutation of Thr42 and Ser337 did not influence USP10's interaction with KRAS, nor did it impair its deubiquitinating activity towards KRAS, while the mutation of Ser76 exerted a weaker deubiquitinating activity towards KRAS due to its impaired enzymatic activity (Fig. S4G), which is consistent with the observation in other study[33], further demonstrating the effect of USP10 on *KRAS* mutants relying on USP10's enzymatic activity. Considering that *KRAS* mutants upregulate USP10 at the posttranslational level rather than the transcriptional level, we tested whether the phosphorylation influences USP10 stability. We found that the co-mutation of Thr42 and Ser337 significantly decreased USP10 stabilization; moreover, overexpression of *KRAS* mutants remarkably increased USP10 stabilization, but this effect was greatly diminished for TA&SA (Fig. 5F).

Taken together, these data demonstrated *KRAS* mutants upregulating USP10 levels and stability by phosphorylating the latter at Thr42 and Ser337.

3.6. *USP10 inhibition preferentially inhibits the growth of KRAS-mutant CRC in vitro and in vivo*

Aforementioned data demonstrated that *USP10* and *KRAS* mutants form a positive feedback circuit. Given the distinct regulatory mechanisms between *USP10* and *KRAS* wild-type/mutants, we speculated that *KRAS*-mutant CRC may be more sensitive to USP10 inhibition. As shown in Fig. 6A and Supporting Information Fig. S5A, depletion of USP10 resulted in a striking reduction of cell growth in *KRAS*-mutant CRC cells, whereas it only exhibited slight effect in *KRAS* wild-type CRC cells. Similar results were observed in the colony formation assay (Fig. 6B), indicating depletion of USP10 preferentially inhibits the proliferation of *KRAS*-mutant CRC cells *in vitro*. To further validate this finding, we conducted *in vivo* xenografts experiments. As presented in Fig. 6C−E, Fig. S5B and Supporting Information Table S5, depletion of USP10 exhibited stronger anti-tumor activity in *KRAS*-mutant CRC xenografts compared to *KRAS* wild-type xenografts.

Collectively, these data underscore the crucial roles of USP10 in *KRAS*-mutant CRC and show that USP10 inhibition preferentially impairs *KRAS*-mutant CRC growth *in vitro* and *in vivo*.

3.7. *USP10 is elevated in KRAS-mutant CRC tissues*

To confirm our findings in a clinical context, we collected *KRAS* wild-type and mutant CRC tissue samples. IHC staining revealed that *KRAS*-mutant CRC tissues exhibit higher USP10 levels compared to *KRAS* wild-type CRC tissues (Fig. 7A−D). Approximately 50% of *KRAS*-mutant CRC patients displayed high (USP10 +++) or medium (USP10 ++) USP10 expression, whereas this population was less than 15% in *KRAS* wild-type patients. These findings further support our conclusion that *KRAS* mutants function as a driver promoting USP10 overexpression in *KRAS*-mutant CRC.

4. Discussion

KRAS is the most frequently mutant driver in human tumors, with approximately 50% of CRC patients harboring *KRAS* mutation. However, existing therapeutic therapies have shown limited efficacy in treating *KRAS*-mutant colorectal cancer. Although $KRAS^{G12C}$ covalent inhibitors have successfully treated patients with this specific mutation, other *KRAS*-mutant tumors with a

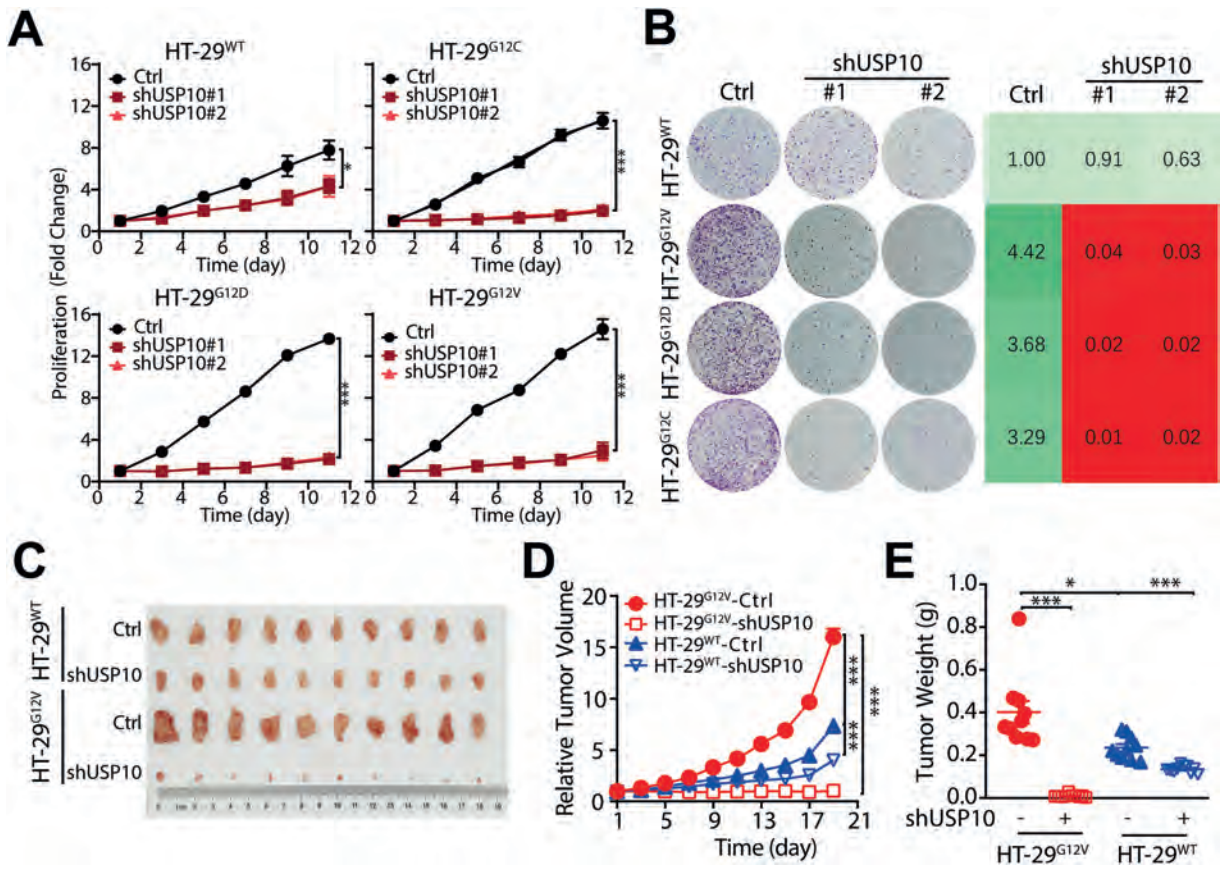

Figure 6 USP10 inhibition preferentially inhibits the growth of *KRAS*-mutant CRC *in vitro* and *in vivo*. (A, B) Depletion of USP10 selectively inhibited *KRAS*-mutant CRC proliferation. HT-29 cells stably expressing $KRAS^{WT/G12C/G12D/G12V}$ were infected with the lentivirus encoding control/USP10 shRNA and then these cells were subjected to cell proliferation assays (A) and colony formation assays (B). (C−E) Depletion of USP10 selectively suppressed *KRAS*-mutant CRC xenografts *in vivo* (mean ± SEM, $n = 10$/group). (C) The tumor images of indicated groups. (D) The relative tumor volume of indicated groups. (E) The tumor weight of indicated groups. $^{*}P < 0.05$; $^{***}P < 0.001$.

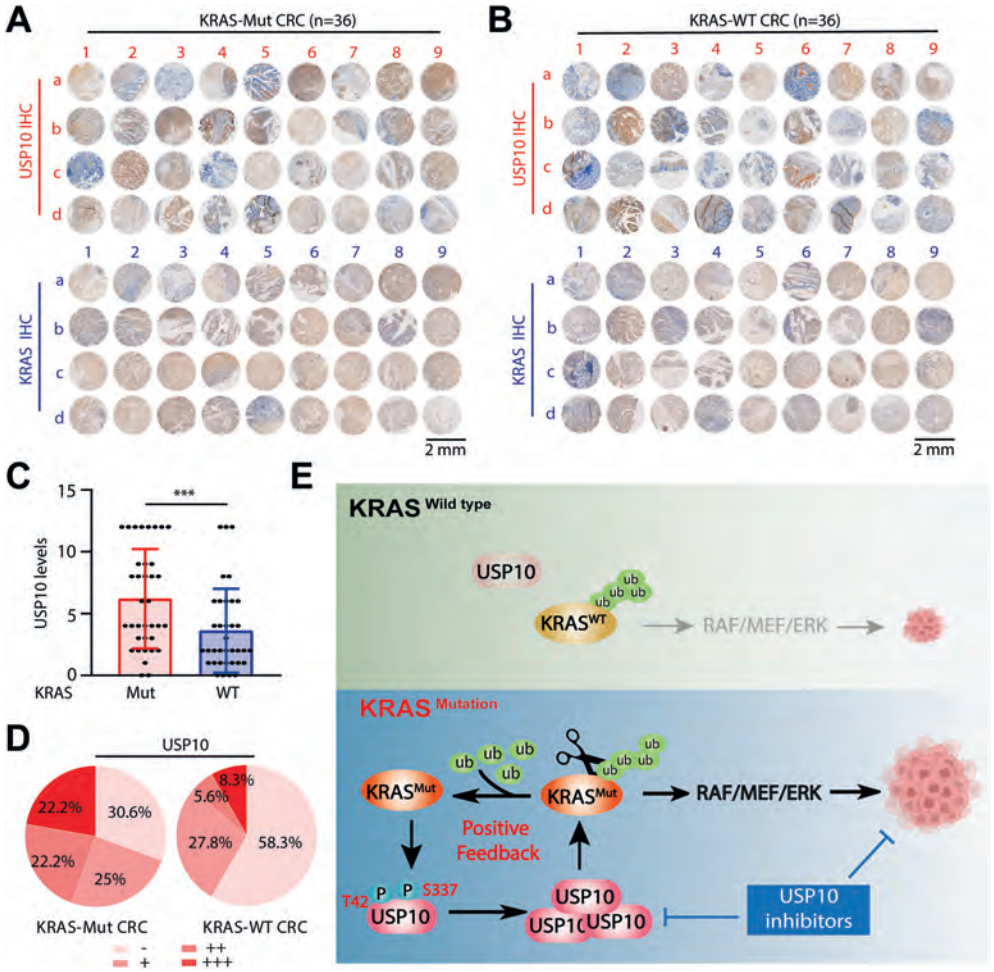

Figure 7 USP10 is elevated in *KRAS*-mutant CRC tissues. (A, B) IHC assays were performed to detect the expression of USP10 and KRAS in *KRAS*-mutant ($n = 36$) and wild-type ($n = 36$) CRC tissues. (C) *KRAS*-mutant CRC tissues displayed higher USP10 levels than *KRAS* wild-type. IHC score was evaluated by multiplication of positive staining proportions (1 score, <25%; 2 score, 25%−50%; 3 score, 50%−75%; 4 score, 75%−100%) and protein expression intensity (1 score, weak staining; 2 score, moderate staining; 3 score, high staining). −, negative expression (1−3 score); +, low expression (4−6 score); ++, medium expression (7−9 score); +++, high expression (10−12 score). (D) Statistical analysis of USP10 expression in *KRAS* wild-type/mutant CRC specimens. (E) The schematic diagram of USP10/KRAS positive feedback circuit promoting the proliferation of *KRAS*-mutant CRC. ***$P < 0.001$.

higher mutation frequency, such as $KRAS^{G12D}$ and $KRAS^{G12V}$, have not benefited from these treatments. Consequently, identifying novel and effective therapeutic targets for these *KRAS*-mutant tumor is of critical importance. In our study, we demonstrated that USP10 depletion preferentially inhibited the growth of *KRAS*-mutant CRC, suggesting USP10 could be a potential therapeutic target for these tumors.

The dysregulation or abnormal activation of DUBs has been widely implicated in tumor progression and malignancy[34-36]. DUBs perform their biological functions by deubiquitinating substrates, thus regulating their abundance, subcellular localization, and activity[37]. Given their well-defined structure and enzymatic sites, DUBs are considered the ideal drug targets. To date, approximately 60 DUB inhibitors have been reported, however, most of these inhibitors are non-selective, targeting multiple DUBs. In our study, through screening DUB inhibitors and LC−MS/MS analysis, we demonstrated that USP10 functions as a crucial DUB regulating the activity of *KRAS* mutants. USP10 belongs to the ubiquitin-specific proteases (USPs), the largest subfamily of DUBs. To date, no specific inhibitors targeting USP10 have been reported and spautin-1 has been reported to inhibit the deubiquitinating activity of both USP10 and USP13[38,39], highlighting the scarcity of specific inhibitors targeting USP10. Therefore, to minimize off-target toxicity, there is an urgent need to develop specific DUB inhibitors for USP10 and other potential DUB targets.

Emerging evidence indicates that ubiquitination modification plays a crucial role in regulating both the abundance and function of KRAS. Yin et al.[16] found that the monoubiquitination of KRAS at lysine 104 alters its conformation and promotes its interaction with guanine nucleotide exchange factors. Another study also reported the monoubiquitination of KRAS at Lys147 and Lys117 promoting the binding affinity between KRAS and PI3K as well as RAF, suggesting that the monoubiquitination of KRAS at Lys104, Lys117 and Lys147 promoted its activity[40]. So far, several E3 ligases, including LZTR1[20,41,42], β-TRCP[21] and WDR76[22], have been reported to regulate KRAS. Despite these findings, the DUBs directly regulating KRAS, particularly the mutant *KRAS*, remain

elusive. A recent study reveals that USP7 deubiquitinates and stabilizes KRAS by removing the K48-linked polyubiquitin chains from residue K147, ultimately promoting non-small cell lung cancer growth[24]. However, the specific DUBs directly regulating *KRAS* mutants' activity without affecting its abundance are still unknown. In our study, we highlight USP10 as a key DUB that modulates KRAS through a direct interaction and maintains the latter's activation. Moreover, we found that the physical association between *USP10* and *KRAS* mutants persists even when USP10's catalytic site is mutated, demonstrating that their protein−protein interaction is independent of USP10's enzymatic activity. In contrast, USP10's ability to reduce KRAS ubiquitination and modulate its activity requires catalytic activity, as USP10-CA fails to deubiquitinate KRAS. This dichotomy is consistent with prior reports for other deubiquitinases[43,44], where substrate binding and enzymatic regulation of DUBs are generally separable events. Although the mutation of the catalytic site does not affect the binding between deubiquitinases and their substrates, the catalytically inactive mutants of DUBs lose their deubiquitinating enzyme activity and cannot effectively remove the ubiquitin chains of substrates, thereby failing to exert any substantial impact on substrates' levels and/or activity.

Polyubiquitination is one of the most important post-translational modifications regulating protein homeostasis and/or activity. K48- and K63-linked polyubiquitination have been widely reported to be involved in proteasomal degradation and DNA repair, and the functions of other non-canonical polyUb chains linked *via* K6-, K11-, K27-, K29-, K33- still need to be further clarified[45]. K6-linked ubiquitination has been demonstrated to control the process of autophagy and DNA damage response; K11-linked ubiquitination is implicated in the regulation of cell cycle and proteasomal degradation; K27-linked ubiquitination functions as a major player of innate immunity by regulating NF-κB and IRF pathways; K29-linked ubiquitination of proteins have been implicated in signaling transduction and neurodegenerative disorders, while K33-linked ubiquitination remains the least studied of all Ub linkage types and may involve in protein trafficking and autophagy regulation[46]. In our study, we found that K6-, K11-, K27-, and K29-linked polyubiquitination mediated KRAS activity, and USP10 promoted KRAS activity by removing these polyubiquitination chains, but the molecular mechanisms and action modes of these types of polyubiquitin chains regulating KRAS activity need to be further investigated in the future.

USP10 exhibits context-dependent roles in tumorigenesis, with its functional duality stemming from substrate specificity and cellular genetic background. Emerging evidence demonstrates that USP10 can act as either an oncogene or a tumor suppressor in different malignancies. For instance, Cao et al.[32] found that USP10 promoted tumor progression by stabilizing mitosis-related protein Anillin (ANLN) in esophageal squamous cell carcinoma. Some lines of evidence reveal the roles of USP10 in modulating the tumor microenvironment, as it could facilitate NF-κB activation through NLR family pyrin domain-containing 7 (NLRP7) deubiquitination, thereby inducing tumor-associated macrophage polarization[47]. Our previous study demonstrated that USP10 promoted hepatocellular carcinoma proliferation by preventing the ubiquitination and degradation of transcription coactivator YAP/TAZ[28]. Conversely, USP10 also exerts tumor-suppressive effect by antagonizing c-Myc through SIRT6 and TP53 stabilization[26], while paradoxically promoting *TP53*-mutant tumor growth despite stabilizing wild-type *TP53*[29]. These studies collectively suggested that USP10's biological consequences are dictated by its substrate repertoire and the molecular landscape of a particular tumor type. In the present study, we identify *KRAS* mutants as key substrates of USP10 in *KRAS*-mutant CRC, where depletion of USP10 selectively inhibited *KRAS*-mutant CRC growth by restraining *KRAS* mutants' activity. Given the dual roles of USP10 in tumors, future development of USP10-targeted therapies should incorporate comprehensive genomics profiling to ensure tumor-specific efficacy.

The roles of USP10 in tumor progression have been extensively documented, yet the mechanisms underlying its high expression in tumors remain ambiguous. In our study, we demonstrated that *KRAS* mutants function as a driver promoting USP10 overexpression in *KRAS*-mutant CRC. Several previous studies have revealed that *KRAS* mutation primarily influences downstream protein regulation through a phosphorylation cascade. *KRAS* mutants-mediated ERK activation promotes the latter's binding and subsequent phosphorylation of F-box and WD repeat domain-containing 7 (FBW7) at Thr205, leading to the degradation of FBW7[48]. Additionally, KRAS mutations are implicated in regulating MYC levels through ERK1/2-mediated phosphorylation of MYC at Ser62[49]. These findings collectively demonstrate that KRAS mutations predominantly modulate protein abundance *via* a phosphorylation cascade. In our study, we have shown that *KRAS* mutations upregulated USP10 protein stability by enhancing its phosphorylation at Thr42 and Ser337. However, the precise mechanisms by which phosphorylation at these specific sites influences USP10's stability are yet to be elucidated and warrant further exploration. Such insights could unlock deeper understanding of KRAS signaling and open new therapeutic avenues for treatment strategies targeting *KRAS*-mutant malignancies, particularly CRC, through modulation of USP10 and the delineated feedback loop.

5. Conclusions

Our study has revealed USP10 as a novel and crucial target for combating *KRAS*-mutant CRC. Mechanistically, USP10 forms an essential part of a positive feedback circuit with *KRAS* mutants, operating through a distinct mechanism in which USP10 directly binds to *KRAS* mutants. It facilitates *KRAS* mutant activation by selectively removing its non-proteolytic ubiquitin chains linked *via* Ub-K6, K11, K27, and K29. This deubiquitination promotes the activation of *KRAS* mutants, which in turn enhances USP10's stability through phosphorylation at Thr42 and Ser 337. The circuit of *USP10*/*KRAS*-mutant is vital, highlighting a synergistic interaction by these two proteins that promotes the growth of *KRAS*-mutant CRC both *in vitro* and *in vivo* (Fig. 7E). Importantly, disrupting this feedback loop using RNA interference against USP10 significantly hinders the growth of *KRAS*-mutant CRC cells, underscoring the pivotal role of the USP10/KRAS feedback mechanism and introducing a promising therapeutic approach for treating *KRAS*-mutant CRC by targeting USP10. This strategy presents a potent avenue for therapeutic intervention, providing a foundational step towards improved treatment outcomes for patients with the challenging mutations of *KRAS*.

Acknowledgements

This work was supported by the Natural Science Foundation of China (U21A20420, 82173836, 82304517), Zhejiang Provincial Natural Science Foundation (LQ23H310009, China).

Author contributions

Conceptualization: Tao Yuan, Weihua Wang, Qiaojun He, Bo Yang, Hong Zhu; Methodology: Tao Yuan, Weihua Wang, Qiaojun He, Bo Yang, Hong Zhu; Investigation: Tao Yuan, Weihua Wang, Ruilin Wu, Yue Liu, Junwei Fu, Jiamin Du, Meijia Qian, Jia'er Wang, Yubo Zhang, Qiaojun He, Bo Yang, Hong Zhu; Visualization: Tao Yuan, Weihua Wang, Qiaojun He, Bo Yang, Hong Zhu; Funding acquisition: Tao Yuan, Bo Yang, Hong Zhu; Project administration: Wencheng Kong, Ronggui Hu, Tianhua Zhou, Qiaojun He, Bo Yang, Hong Zhu; Supervision: Wencheng Kong, Ronggui Hu, Tianhua Zhou; Writing − original draft: Tao Yuan, Weihua Wang, Qiaojun He, Bo Yang, Hong Zhu; Writing − review & editing: Tao Yuan, Qiaojun He, Bo Yang, Hong Zhu.

Conflicts of interest

The authors declare no conflicts of interest.

Appendix A. Supporting information

Supporting information to this article can be found online at https://doi.org/10.1016/j.apsb.2025.11.015.

References

1. Kao AT, Cabanlong CV, Padilla K, Xue X. Unveiling ferroptosis as a promising therapeutic avenue for colorectal cancer and colitis treatment. *Acta Pharm Sin B* 2024;**14**:3785−801.
2. Kuppusamy P, Yusoff MM, Maniam GP, Ichwan SJ, Soundharrajan I, Govindan N. Nutraceuticals as potential therapeutic agents for colon cancer: a review. *Acta Pharm Sin B* 2014;**4**:173−81.
3. Siegel RL, Miller KD, Goding SA, Fedewa SA, Butterly LF, Anderson JC, et al. Colorectal cancer statistics, 2020. *CA Cancer J Clin* 2020;**70**:145−64.
4. Biller LH, Schrag D. Diagnosis and treatment of metastatic colorectal cancer: a review. *JAMA* 2021;**325**:669−85.
5. Dekker E, Tanis PJ, Vleugels JLA, Kasi PM, Wallace MB. Colorectal cancer. *Lancet* 2019;**394**:1467−80.
6. Cox AD, Fesik SW, Kimmelman AC, Luo J, Der CJ. Drugging the undruggable RAS: mission possible?. *Nat Rev Drug Discov* 2014;**13**: 828−51.
7. Wang WH, Yuan T, Qian MJ, Yan FJ, Yang L, He QJ, et al. Post translational modification of KRAS: potential targets for cancer therapy. *Acta Pharmacol Sin* 2021;**42**:1201−11.
8. Wang Y, Zhang Y, Luo H, Wei W, Liu W, Wang W, et al. Identification of USP2 as a novel target to induce degradation of KRAS in myeloma cells. *Acta Pharm Sin B* 2024;**14**:5235−48.
9. Feng J, Lian Z, Xia X, Lu Y, Hu K, Zhang Y, et al. Targeting metabolic vulnerability in mitochondria conquers MEK inhibitor resistance in *KRAS*-mutant lung cancer. *Acta Pharm Sin B* 2023;**13**:1145−63.
10. Hong DS, Fakih MG, Strickler JH, Desai J, Durm GA, Shapiro GI, et al. *KRAS*(G12C) inhibition with sotorasib in advanced solid tumors. *N Engl J Med* 2020;**383**:1207−17.
11. Weiss A, Lorthiois E, Barys L, Beyer KS, Bomio CC, Burks H, et al. Discovery, preclinical characterization, and early clinical activity of JDQ443, a structurally novel, potent, and selective covalent oral inhibitor of KRASG12C. *Cancer Discov* 2022;**12**:1500−17.
12. Hallin J, Engstrom LD, Hargis L, Calinisan A, Aranda R, Briere DM, et al. The KRAS(G12C) inhibitor MRTX849 provides insight toward therapeutic susceptibility of *KRAS*-mutant cancers in mouse models and patients. *Cancer Discov* 2020;**10**:54−71.
13. Awad MM, Liu S, Rybkin II, Arbour KC, Dilly J, Zhu VW, et al. Acquired resistance to KRAS(G12C) inhibition in cancer. *N Engl J Med* 2021;**384**:2382−93.
14. Akhave NS, Biter AB, Hong DS. Mechanisms of resistance to KRAS (G12C)-targeted therapy. *Cancer Discov* 2021;**11**:1345−52.
15. Zhao Y, Murciano GYR, Xue JY, Ang A, Lucas J, Mai TT, et al. Diverse alterations associated with resistance to KRAS(G12C) inhibition. *Nature* 2021;**599**:679−83.
16. Yin G, Zhang J, Nair V, Truong V, Chaia A, Petela J, et al. KRAS ubiquitination at lysine 104 retains exchange factor regulation by dynamically modulating the conformation of the interface. *iScience* 2020;**23**:101448.
17. Nair VV, Yin G, Zhang J, Hancock JF, Campbell SL, Gorfe AA. Monoubiquitination of KRAS at Lys104 and Lys147 modulates its dynamics and interaction with partner proteins. *J Phys Chem B* 2021; **125**:4681−91.
18. Bard JAM, Goodall EA, Greene ER, Jonsson E, Dong KC, Martin A. Structure and function of the 26S proteasome. *Annu Rev Biochem* 2018;**87**:697−724.
19. Harrigan JA, Jacq X, Martin NM, Jackson SP. Deubiquitylating enzymes and drug discovery: emerging opportunities. *Nat Rev Drug Discov* 2018;**17**:57−78.
20. Bigenzahn JW, Collu GM, Kartnig F, Pieraks M, Vladimer GI, Heinz LX, et al. LZTR1 is a regulator of RAS ubiquitination and signaling. *Science* 2018;**362**:1171−7.
21. Kim SE, Yoon JY, Jeong WJ, Jeon SH, Park Y, Yoon JB, et al. H-Ras is degraded by Wnt/β-catenin signaling *via* β-TrCP-mediated polyubiquitylation. *J Cell Sci* 2009;**122**:842−8.
22. Jeong WJ, Park JC, Kim WS, Ro EJ, Jeon SH, Lee SK, et al. WDR76 is a RAS binding protein that functions as a tumor suppressor *via* RAS degradation. *Nat Commun* 2019;**10**:295.
23. Baietti MF, Simicek M, Abbasi Asbagh L, Radaelli E, Lievens S, Crowther J, et al. OTUB1 triggers lung cancer development by inhibiting RAS monoubiquitination. *EMBO Mol Med* 2016;**8**: 288−303.
24. Huang B, Cao D, Yuan X, Xiong Y, Chen B, Wang Y, et al. USP7 deubiquitinates KRAS and promotes non-small cell lung cancer. *Cell Rep* 2024;**43**:114917.
25. Wang X, Xia S, Li H, Wang X, Li C, Chao Y, et al. The deubiquitinase USP10 regulates KLF4 stability and suppresses lung tumorigenesis. *Cell Death Differ* 2020;**27**:1747−64.
26. Lin Z, Yang H, Tan C, Li J, Liu Z, Quan Q, et al. USP10 antagonizes c-Myc transcriptional activation through SIRT6 stabilization to suppress tumor formation. *Cell Rep* 2013;**5**:1639−49.
27. Weisberg EL, Schauer NJ, Yang J, Lamberto I, Doherty L, Bhatt S, et al. Inhibition of USP10 induces degradation of oncogenic FLT3. *Nat Chem Biol* 2017;**13**:1207−15.
28. Zhu H, Yan F, Yuan T, Qian M, Zhou T, Dai X, et al. USP10 promotes proliferation of hepatocellular carcinoma by deubiquitinating and stabilizing YAP/TAZ. *Cancer Res* 2020;**80**:2204−16.
29. Yuan J, Luo K, Zhang L, Cheville JC, Lou Z. USP10 regulates p53 localization and stability by deubiquitinating p53. *Cell* 2010;**140**: 384−96.
30. Yuan T, Zeng C, Liu J, Zhao C, Ge F, Li Y, et al. Josephin domain containing 2 (JOSD2) promotes lung cancer by inhibiting LKB1 (liver kinase B1) activity. *Signal Transduct Targeted Ther* 2024;**9**:11−26.
31. Liu X, Zhang S, An Y, Xu B, Yan G, Sun M. USP10/XAB2/ANXA2 axis promotes DNA damage repair to enhance chemoresistance to oxaliplatin in colorectal cancer. *J Exp Clin Cancer Res* 2025;**44**:94.
32. Cao YF, Xie L, Tong BB, Chu MY, Shi WQ, Li X, et al. Targeting USP10 induces degradation of oncogenic ANLN in esophageal squamous cell carcinoma. *Cell Death Differ* 2023;**30**:527−43.
33. Deng M, Yang X, Qin B, Liu T, Zhang H, Guo W, et al. Deubiquitination and activation of AMPK by USP10. *Mol Cell* 2016;**61**:614−24.
34. Li C, Xia J, Franqui-Machin R, Chen F, He Y, Ashby TC, et al. TRIP13 modulates protein deubiquitination and accelerates tumor development and progression of B cell malignancies. *J Clin Investig* 2021;**131**:e146893.
35. Qian M, Yan F, Wang W, Du J, Yuan T, Wu R, et al. Deubiquitinase JOSD2 stabilizes YAP/TAZ to promote cholangiocarcinoma progression. *Acta Pharm Sin B* 2021;**11**:4008−19.

36. Qian M, Yan F, Wang W, Du J, Yuan T, Wu R, et al. Deubiquitinase JOSD2 stabilizes YAP/TAZ to promote cholangiocarcinoma progression. *Acta Pharm Sin B* 2021;**11**:4008−19.
37. Yuan T, Yan F, Ying M, Cao J, He Q, Zhu H, et al. Inhibition of ubiquitin-specific proteases as a novel anticancer therapeutic strategy. *Front Pharmacol* 2018;**9**:1080−9.
38. Liu J, Xia H, Kim M, Xu L, Li Y, Zhang L, et al. Beclin1 controls the levels of p53 by regulating the deubiquitination activity of USP10 and USP13. *Cell* 2011;**147**:223−34.
39. Guo J, Zhang J, Liang L, Liu N, Qi M, Zhao S, et al. Potent USP10/13 antagonist spautin-1 suppresses melanoma growth *via* ROS-mediated DNA damage and exhibits synergy with cisplatin. *J Cell Mol Med* 2020;**24**:4324−40.
40. Sasaki AT, Carracedo A, Locasale JW, Anastasiou D, Takeuchi K, Kahoud ER, et al. Ubiquitination of K-Ras enhances activation and facilitates binding to select downstream effectors. *Sci Signal* 2011;**4**: ra13.
41. Steklov M, Pandolfi S, Baietti MF, Batiuk A, Carai P, Najm P, et al. Mutations in *LZTR1* drive human disease by dysregulating RAS ubiquitination. *Science* 2018;**362**:1177−82.
42. Abe T, Umeki I, Kanno SI, Inoue SI, Niihori T, Aoki Y. LZTR1 facilitates polyubiquitination and degradation of RAS-GTPases. *Cell Death Differ* 2020;**27**:1023−35.
43. Qiu W, Xiao Z, Yang Y, Jiang L, Song S, Qi X, et al. USP10 deubiquitinates RUNX1 and promotes proneural-to-mesenchymal transition in glioblastoma. *Cell Death Dis* 2023;**14**:207.
44. Yuan T, Liu Y, Wu R, Qian M, Wang W, Li Y, et al. Josephin domain containing 2 (JOSD2) inhibition as pan-*KRAS*-mutation-targeting strategy for colorectal cancer. *Nat Commun* 2025;**16**: 3623.
45. Castañeda CA, Dixon EK, Walker O, Chaturvedi A, Nakasone MA, Curtis JE, et al. Linkage *via* K27 bestows ubiquitin chains with unique properties among polyubiquitins. *Structure* 2016;**24**:423−36.
46. Tracz M, Bialek W. Beyond K48 and K63: non-canonical protein ubiquitination. *Cell Mol Biol Lett* 2021;**26**:1.
47. Li B, Qi ZP, He DL, Chen ZH, Liu JY, Wong MW, et al. NLRP7 deubiquitination by USP10 promotes tumor progression and tumor-associated macrophage polarization in colorectal cancer. *J Exp Clin Cancer Res* 2021;**40**:126.
48. Ji S, Qin Y, Shi S, Liu X, Hu H, Zhou H, et al. ERK kinase phosphorylates and destabilizes the tumor suppressor FBW7 in pancreatic cancer. *Cell Res* 2015;**25**:561−73.
49. Vaseva AV, Blake DR, Gilbert TSK, Ng S, Hostetter G, Azam SH, et al. KRAS suppression-induced degradation of MYC is antagonized by a MEK5-ERK5 compensatory mechanism. *Cancer Cell* 2018;**34**: 807−22.